Microstructural Evolution in the HAZ of Inconel 718 and Correlation with the Hot Ductility Test

The results of hot ductility tests indicate that heat treatment significantly alters the hot cracking susceptibility of alloy 718

BY R. G. THOMPSON AND S. GENCULU

ABSTRACT. The nickel-base alloy 718 was evaluated to study the role of preweld heat treatment in reducing or eliminating heat-affected zone hot cracking. Three heat treatments were studied using the Gleeble hot ductility test. A modified hot ductility test was also used to follow the evolution of microstructure during simulated welding thermal cycles. The microstructural evolution was correlated with the hot ductility data in order to evaluate the mechanism of hot cracking in alloy 718.

The correlation of hot ductility with microstructure showed that recrystallization, grain growth, and dissolution of precipitates did not in themselves cause any loss of ductility during cooling. Ductility loss during cooling was not initiated until the constitutional liquation of NbC particles was observed in the microstructure. Laves-type phases were found precipitated in the solidified grain boundaries but were not found to correlate with any ductility loss parameter.

Mechanisms are reviewed which help to explain how heat treatment controls the hot crack susceptibility of alloy 718 as measured in the hot ductility test.

Introduction

The hot ductility test is often used to evaluate a metal's susceptibility to heat-affected zone (HAZ) hot cracking. The test consists of a thermal cycle, including both heating and cooling, which is imposed on the metal to simulate the HAZ conditions of a given welding process (Ref. 1). The metal is fractured at a predetermined point in the thermal cycle to test the mechanical response of the HAZ microstructure. Data from these tests are plotted as ductility versus temperature. The hot ductility response of many metals during the heating portion of the thermal cycle appears to have several features in common; these are:

1. Rapid loss of ductility with the onset of intergranular fracture.
2. A nil ductility temperature (NDT) characteristic of the material.
3. A nil strength temperature (NST) roughly corresponding to the metal's bulk solidus temperature.

The hot ductility response of a metal during cooling from the peak HAZ temperature is usually considered indicative of its susceptibility to hot cracking (Ref. 2). If the metal regains its ductility over a short temperature range, it is usually insensitive to HAZ hot cracking. If the metal's ductility remains close to zero over a wide temperature range on cooling, it is usually hot-crack sensitive. Such observations have been reported previously for various nickel base alloys (Refs. 2-4). (Kreischer [Ref. 5] has reported another interpretation criteria for certain stainless steels based on the recovery of tensile strength during cooling rather than ductility.)

Hot crack susceptibility varies greatly in various alloys, and the identification of the mechanisms responsible for HAZ hot crack susceptibility is a primary concern. Alloy chemistry and microstructure have been an intense area of study relative to hot crack susceptibility. Weiss, Grotke and Stickler (Ref. 4) proposed that constitutional liquation of intergranular precipitates in Inconel 600 resulted in an intergranular failure mode and loss of both ductility and strength. They concluded that hot cracking resulted from intergranular wetting by the liquated precipitates.

Yeniscavich (Ref. 3) reached conclusions similar to Weiss *et al.* in studies of EN 82 filler metal used with Inconel 600 base metal. A primary difference between these two studies involved the liquation mechanism. Yeniscavich proposed a eutectic-melting intergranular phase chemistry which remained molten during cooling well below the bulk solidus temperature. Owczarski, Duvall and Sullivan (Ref. 6) studied Udimet 700 and Waspaloy employing the hot ductility technique. They, like Weiss *et al.* and Yeniscavich, found incipient intergranular melting to be associated with enhanced hot crack susceptibility. They concluded that constitutional liquation of MC-type carbides resulted in intergranular liquid. However, unlike the above mentioned studies, Owczarski *et al.* concluded liquation did not begin until above the NDT on heating. The initial loss of ductility on heating and intergranular fracture mode were suggested to be intrinsic material characteristics reminiscent of the equicohesive temperature and thus dependent on both material and test variables.

Partial intergranular melting, similar to that reported in the hot ductility literature, has been observed and reported for a number of alloys. Partial melting in the region adjacent to the weld fusion zone has been described for cupronickel (Ref. 7), Inconel 600 (Refs. 8, 9), and HY-80 (Refs. 10, 11). The relationship of this zone to hot crack sensitivity has been investigated with respect to a number of minor alloying and tramp elements in Inconel 600 (Refs. 8, 9) and cupronickel (Ref. 12). It was found that elements such as sulfur and phosphorus increased hot crack susceptibility through their influence on the solid-liquid interfacial energy (Ref. 8), *i.e.*, wetting angle. Studies by Savage, Nippes and Mushala (Refs. 13,

Paper presented at the 64th Annual AWS Convention held in Philadelphia, Pennsylvania, during April 24-29, 1983.

R. G. THOMPSON, Assistant Professor, and S. GENCULU, Graduate Student, are with the Department of Materials Engineering, School of Engineering, The University of Alabama, Birmingham, Alabama.

14) have also investigated the role of copper-rich intergranular liquid in hot crack susceptibility. These studies point out the universal nature of the relationship between intergranular liquid formation and HAZ hot cracking.

It is now well established that the susceptibility to HAZ hot cracking is related to the development of an intergranular liquid phase in the HAZ during welding. The interrelationship between liquid and hot cracking naturally suggests a review of solidification cracking literature. Papers by Pumphrey and Jennings (1948) (Ref. 15), C. S. Smith (1948) (Ref. 16), W. M. Williams and Smith (1952) (Ref. 17), J. A. Williams and Singer (1966) (Ref. 18) and Borland (1979) (Ref. 19) help summarize the recent history of research on solidification cracking.

It is readily seen that research on solidification cracking has centered on the role of intergranular liquid in the cracking process. The approach pioneered by Smith (Ref. 16) and most often used to describe the distribution of intergranular liquid is the dihedral angle. The dihedral angle that the intergranular liquid makes with the bulk solid has been shown to correlate with cracking (Ref. 20) and be a function of temperature (Refs. 18, 21-23), stress (Refs. 23, 24), and trace elements (Ref. 21). Note that these variables, with the exception of stress, have also been shown to control HAZ hot cracking. It might be anticipated that the susceptibility to HAZ hot cracking is dependent on the distribution of intergranular liquid. Thus, the existence of intergranular liquid does not in itself constitute a hot crack sensitive condition unless it is distributed in a detrimental manner.

The nickel-base alloy 718* is the subject of the present investigation. It has also been the subject of various studies which examined both its physical metallurgy characteristics (Ref. 25) and its susceptibility to HAZ hot cracking (Refs. 2, 26). E. G. Thompson (Ref. 26) studied several heats of 718 which had different mill practices and heat treatments. He showed that heat-to-heat chemistry differences, mill practice, and heat treatment all produced changes in alloy 718's susceptibility to hot cracking. He concluded that intergranular liquid films, resulting from molten Laves phase, were responsible for an increased susceptibility to hot cracking. It was also felt that boron, carbides, and/or silicides might also play a role in the observed hot cracking.

Duvall and Owczarski (Ref. 2) also studied the hot crack susceptibility of 718. They found that both solution annealed and fully heat treated 718 began to melt when heated to the alloy's NST. Initial liquation was observed both intragranularly and intergranularly adjacent to niobium-rich MC-type carbides. Welding hot cracks in Inconel 718 have been studied by R. Vincent (Ref. 27) using convergent beam electron diffraction and energy dispersive x-ray techniques. He found that HAZ cracks were intimately associated with NbC carbides and Laves phase. The Laves phase was an AB_2 hexagonal type with an atomic composition of 29% Nb and 65% Ni, Cr, and Fe.

The studies on 718 indicate that hot cracking susceptibility is intimately related to the formation of intergranular liquid films in a manner similar to that proposed for other alloys. Studies on Inconel 718 also defined the importance of its second phase microstructure on the development of the intergranular liquid.

Previous studies have examined the microstructure-hot ductility relationship through postmortem evaluation of specimens whose microstructure was characteristic of the specimen's cooling rate rather than any particular ductility measure. This has been true for alloy 718 in both simulated welding conditions using the hot ductility test and in prototype welds. The present paper presents a study of microstructural evolution and correlates this to hot ductility data. This was done for three preweld microstructures from a single 718 heat. Such an approach helps to explain some observations made on postmortem microstructures and also ties together information from previous studies on the role of microstructural interactions in hot cracking.

Experimental Procedure

A Gleeble 510 was used to generate a simulated welding thermal cycle typical of that found in the HAZ of 1½ in. (38.1 mm) thick stainless steel with an energy input of 70,000 joules/in. (2,756,000 J/m) (Ref. 2, 26). This thermal cycle was imposed on 718 filler metal of the composition given in Table 1. This was tested in the as-received, solution annealed, and age hardened conditions as given in Table 2. All tests were performed in air. The small diameter — 0.061 in. (1.5 mm) — filler metal helped to facilitate the rapid quench rates desired for microstructural evaluation.

Hot ductility curves were generated in the usual way (Ref. 2) using the 0.061 in. (1.5 mm) diameter filler metal as the test specimen with a 1.0 in. (25.4 mm) length of specimen between the grips. Microstructures were developed to correspond with the hot ductility data points in the following manner. A specimen was thermally cycled in the Gleeble as if a hot ductility test was being made. However, instead of the fracture event occurring at a predetermined temperature, the specimen was rapidly quenched to preserve the microstructure. Quenching was accomplished by stopping the current flow to the specimen and simultaneously inundating the specimen with water. The effect of this quench procedure on cooling rate is compared to other cooling rates obtained using non-quench procedures in Fig. 1.

Microstructures developed by the imposed cycle were revealed by mechanically polishing the samples through 0.3 micron (0.0003 mm or 0.000012 in.) and etching. The as-received specimens were etched by swabbing with Kalling's reagent. The solution annealed and age-hardened specimens were electrolytically etched in oxalic acid at 5 V and 0.2 A for 5 seconds(s).

Energy dispersive x-ray analysis was performed using a standardless program with the Edax 9100 system and a Cambridge model 150 scanning electron microscope.

Table 1—Chemical Analysis of Alloy 718, %

Cr	18.15	S	0.005
Ni	52.15	Mo	3.01
Fe	Bal.	Al	0.52
C	0.052	V	0.09
Si	0.08	Cu	0.04
Nb + Ta	5.12	B	0.003
Mn	0.14	Ti	1.00
P	0.005	N_2	0.01

Results

The as-received (AR) material (Fig. 2A) exhibited a loss of ductility over a wide temperature range during cooling from peak temperatures found in the heat-affected zone (HAZ). Other studies (Refs. 2-4) on nickel alloys have shown that this

Table 2—Schedule of Heat Treating

Alloy condition	Heat treatment[a]
As-received (AR)	Vacuum annealed at 1950-2000°F and cold drawn (this step repeated several times)
Solution annealed (SA)	AR plus; vacuum annealed at 1750°F for 1 h and furnace cooled
Age hardened (AH)	SA plus: vacuum aged at 1400°F for 8 h, furnace cooled to 1200°F, held for 10 h and furnace cooled

(a) °C = (5/9) (°F −32)

Also known as Inconel 718.

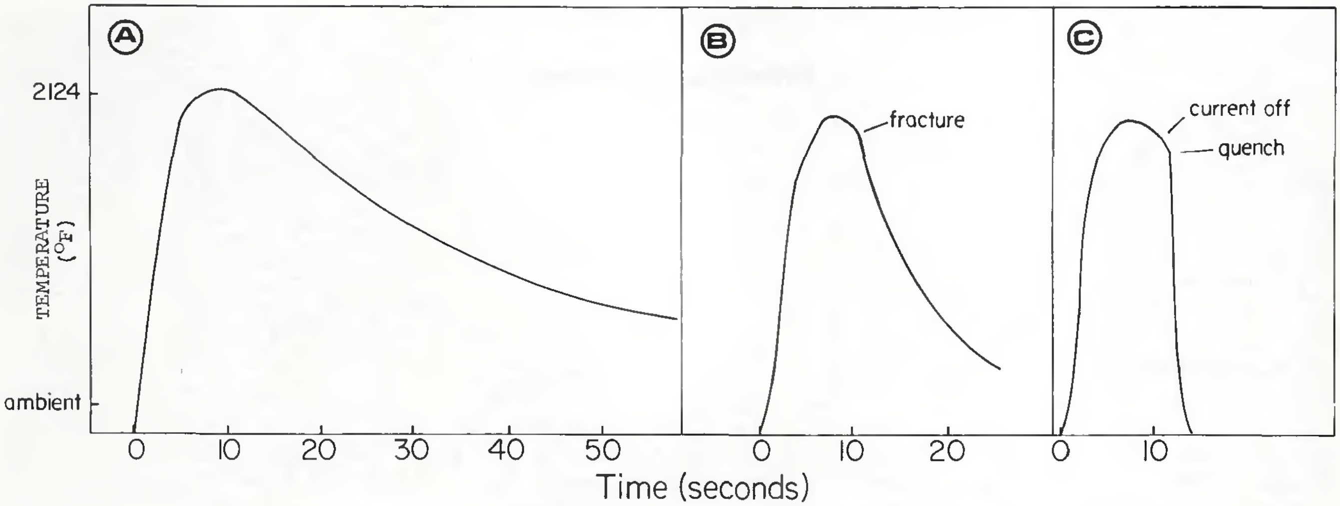

Fig. 1 — Comparison of cooling rates from three hot ductility test conditions: A — programmed thermal cycle (see Experimental Procedure); B — cooling rate of fractured hot ductility test specimen; C — cooling rate of specimen using quench technique of current study

is indicative of a metal which is susceptible to HAZ hot cracking during welding.

The age-hardened (AH) material (Fig. 2C) regained ductility at a higher temperature than did the AR condition and should be less sensitive to HAZ cracking. The solution annealed (SA) heat treatment (Fig. 2B) resulted in a microstructure which regained ductility very rapidly on cooling. Based solely on the hot ductility test results, it would be expected that the SA microstructure was more resistant to HAZ hot cracking than the other microstructures studied.

On-Heating Ductility Loss

The loss of ductility during heating was similar in all three heat treatments, although the microstructural changes which occurred during heating were quite different. Figure 3 shows the recrystallization and grain growth sequence typical of the cold worked, AR condition. The only microstructural change observed in the AR condition during the ductility loss on heating was grain

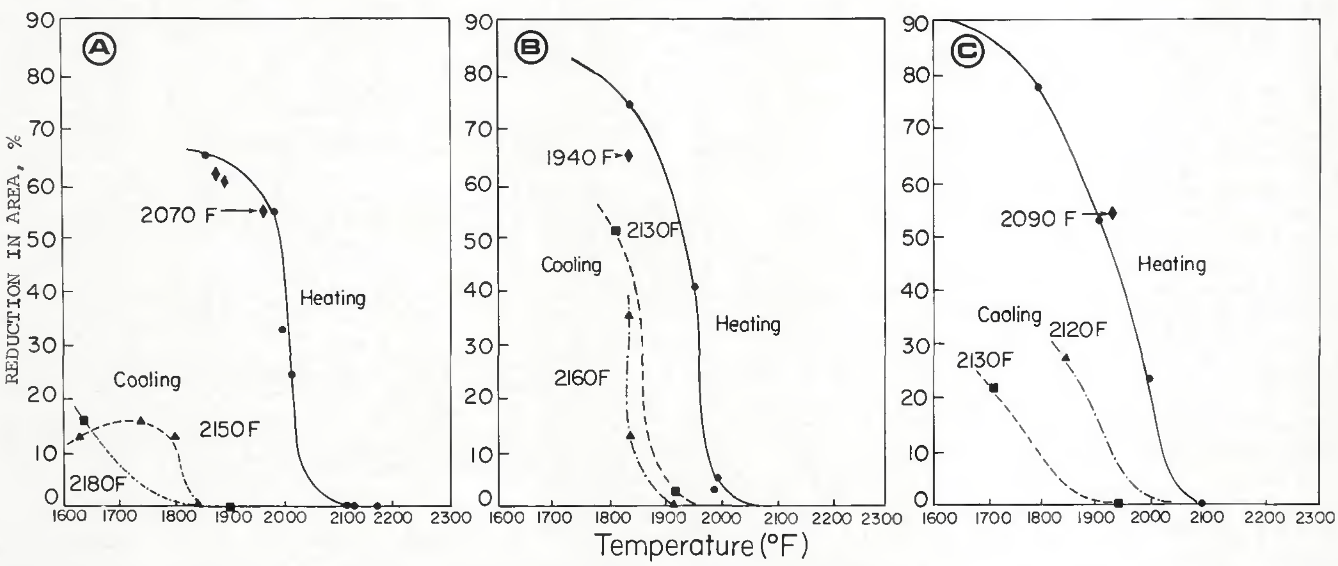

Fig. 2 — Hot ductility dependence on heat treatment for Inconel 718: A — hot ductility curves for as-received 718; B — hot ductility curves for solution-annealed 718; C — hot ductility curves for age-hardened 718. Heating — (●); cooling — (♦, ■, ▲)

Fig. 3 — Recrystallization in as-received 718: A — initial recrystallization in cold worked structure; B — fully recrystallized structure; C — recrystallized structure evidencing subsequent grain growth

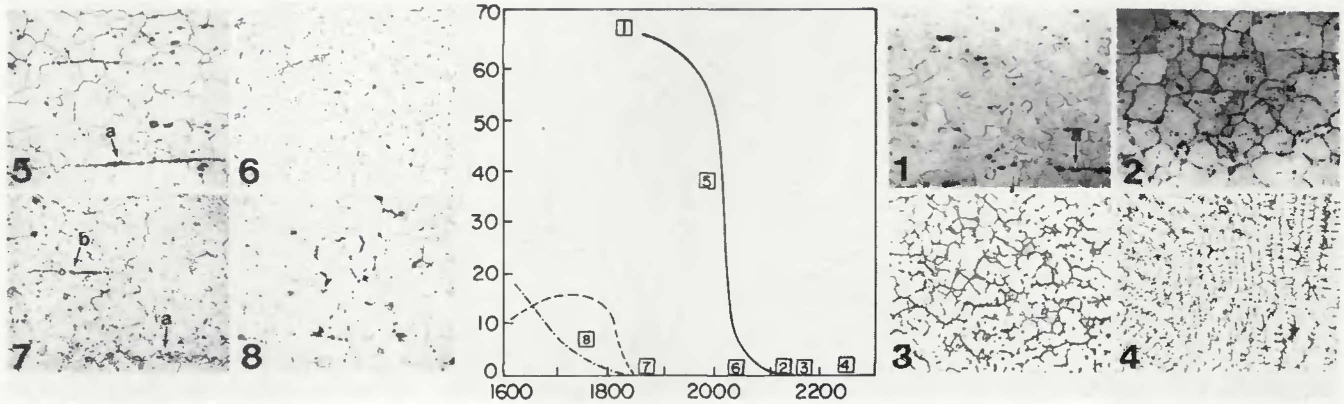

Fig. 4—Microstructural evolution in as-received 718 during hot ductility test: 1. Quenched during heating at 1850°F, 2. Quenched during heating at 2120°F, 3. Quenched during heating at 2190°F, 4. Quenched during heating at 2280°F, 5. Quenched during cooling at 2035°F from a maximum temperature of 2060°F, 6. Quenched during cooling at 2080°F from 2125°F, 7. Quenched during cooling at 1890°F from 2190°F, 8. Quenched during cooling at 1760°F from 2170°F. °C = 5/9 (°F-32)

growth. Intergranular melting was observed in the AR condition but not until the nil ductility temperature (NDT) (~2100 F) had been exceeded. This sequence is shown in Fig. 4.

The microstructural evolution during heating in the SA and AH 718 was quite different from that described for the AR material. The recrystallization and grain growth observed in the AR condition did not occur during tests on the SA and AH material. This was expected since the thermally activated recrystallization of the cold worked, AR material would have taken place during the heat treating of the SA and AH materials. Also, the SA and AH heat treatments produced a strong precipitation of a coarse Ni_3Nb phase. This phase was identified by energy dispersive x-ray (Table 3) and examination of the TTT diagram (Refs. 25, 27) (Fig. 5) for 718.

It was also expected that γ', γ'' were precipitated during these heat treatments as evidenced by the increases in hardness exhibited after heat treatment. It was, however, beyond the scope of the present study to follow the evolution of microconstituents which required transmission electron microscopy for identification.

Figure 6 shows the dissolution of the Ni_3Nb phase during heating. This was typical for both the SA and AH conditions. Figures 7 and 8 also show this behavior in relation to the hot ductility test curves. The dissolution of these precipitates appeared to have little or no effect on the ductility during heating. In particular, their dissolution did not appear to affect the onset of ductility loss, the rate of ductility loss with respect to temperature, or the NDT.

The SA and AH microstructures both exhibited grain boundary liquation above the NDT. This behavior was similar to the AR condition as seen in Figs. 9-11.

Table 3—Energy Dispersive X-ray Analysis of Microstructures (Figs. 4, 6-11)

Constituent(a)	Nb	Mo	Ti	Ni	Cr	Fe	Si	5	Al
a (NbC)	85.0	1.5	5.6	1.4	0.6	0.6	2.9	0.0	2.5
b (TiC)	11.9	0.1	82.5	0.6	0.9	0.5	0.7	0.0	2.8
c (Ni_3Nb)	12.7	2.0	1.6	52.7	13.5	11.7	0.8	0.2	4.9
d (Laves)	21.7	3.4	2.0	44.4	12.6	9.9	1.3	0.8	3.9
e (G.B. Region)	8.7	2.6	1.1	49.5	17.3	15.5	0.8	0.6	3.9
f (Matrix)	4.3	2.2	0.8	51.6	18.8	16.6	0.7	0.6	4.4

(a) Constituents a and b showed little variation in chemistry; c varied with size of particle analyzed; d varied in Nb content from 19.4 to 23.5; e varied in Nb content from 7.2 to 16.6; f varied in Nb content from 2.5 in the AR to 4.3 in the SA.

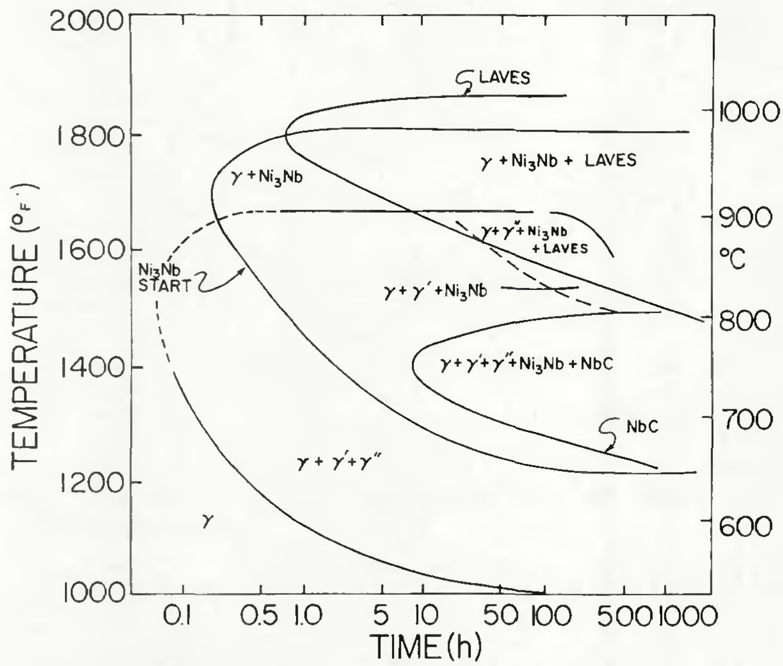

Fig. 5—Transformation diagram for Inconel 718 (Ref. 27)

On-Cooling Ductility

It was found that several microstructural changes had no apparent effect on ductility. Figure 2 shows that no ductility was lost on cooling from a maximum temperature approximately equal to the NDT (~2100°F or 1150°C). The hot ductility data, when considered with Figs. 4, 7, and 8 suggest that incipient melting was a prerequisite for on-cooling ductility loss in alloy 718. The data also show that neither recrystallization and grain growth nor dissolution of the Ni_3Nb precipitates cause a ductility loss during cooling in the absence of intergranular melting.

The degree of ductility loss during cooling in alloy 718 increased in proportion to the volume of intergranular liquid formed during heating. This relationship is evidenced in Fig. 4. As the maximum temperature was raised above the incipient melting temperature, the volume of intergranular liquid increased until bulk melting consumed the microstructure. Figures 7 and 8 show the same behavior

Fig. 6 — Dissolution of Ni_3Nb platelet streaks during heating: A — precipitate streaks typical of both the solution annealed and the age hardened microstructures; B — platelet morphology of Ni_3Nb particles which constitute the precipitate streaks seen in A; C — Ni_3Nb platelets of B seen in initial stage of dissolution during heating

for the SA and AH conditions. When Figures 4, 7, and 8 are compared with Fig. 2, the following observation can be made: the higher the metal was heated above the incipient melting temperature, the greater was the volume of intergranular liquid and the more prolonged was its loss of ductility on cooling.

Figures 9–11 show the development of intergranular liquid in the three heat treatments studied. Table 3 lists the chemical compositions of the phases identified with labels in Figs. 4, 6-11.

Note that the resolution of the chemical analysis techniques restricted the phases which could be identified. For example, no Laves phase was detected in the pre-test microstructure although it would be expected from the TTT diagram (Ref. 25, 27) and other 718 studies (Ref. 26, 27).

All three heat-treated conditions appeared to experience the same process of constitutional liquation from NbC precipitates. Note that the TiC precipitates remained unchanged during the liquation of the NbC particles. The identification of Laves-type precipitates (Ni, Cr, Fe)$_2$ (Nb, Mo, Ti) in the widened grain boundaries was also found in all three heat treated conditions. Table 4 is a summary of phases identifiable in the present study and their observed interaction with the intergranular liquid phase.

Figures 4, and 7-11 suggest that at the temperature of incipient melting the microstructures of all three heat treatments formed the intergranular liquid phase in the same manner. This behavior is interesting in light of the wide disparity in ductility exhibited during the cooling of these liquated microstructures.

This disparity is not clearly seen in Fig. 2. A more dramatic measure of ductility loss due to heat treatment can be constructed based on relative temperature differences. Consider Fig. 12. The temperature difference ΔT_{NDT} gives the magnitude of ductility loss during cooling relative to the NDT for each maximum temperature used. Since ΔT_{NDT} is a function of the maximum temperature, ΔT_{NDT} should be correlated to a variable related to this maximum temperature. Such a variable is the temperature difference (ΔT_{NbC}) between the incipient melting of the NbC particle and the maximum temperature. ΔT_{NbC} is important, because it is a relative measure of the extent of intergranular melting.

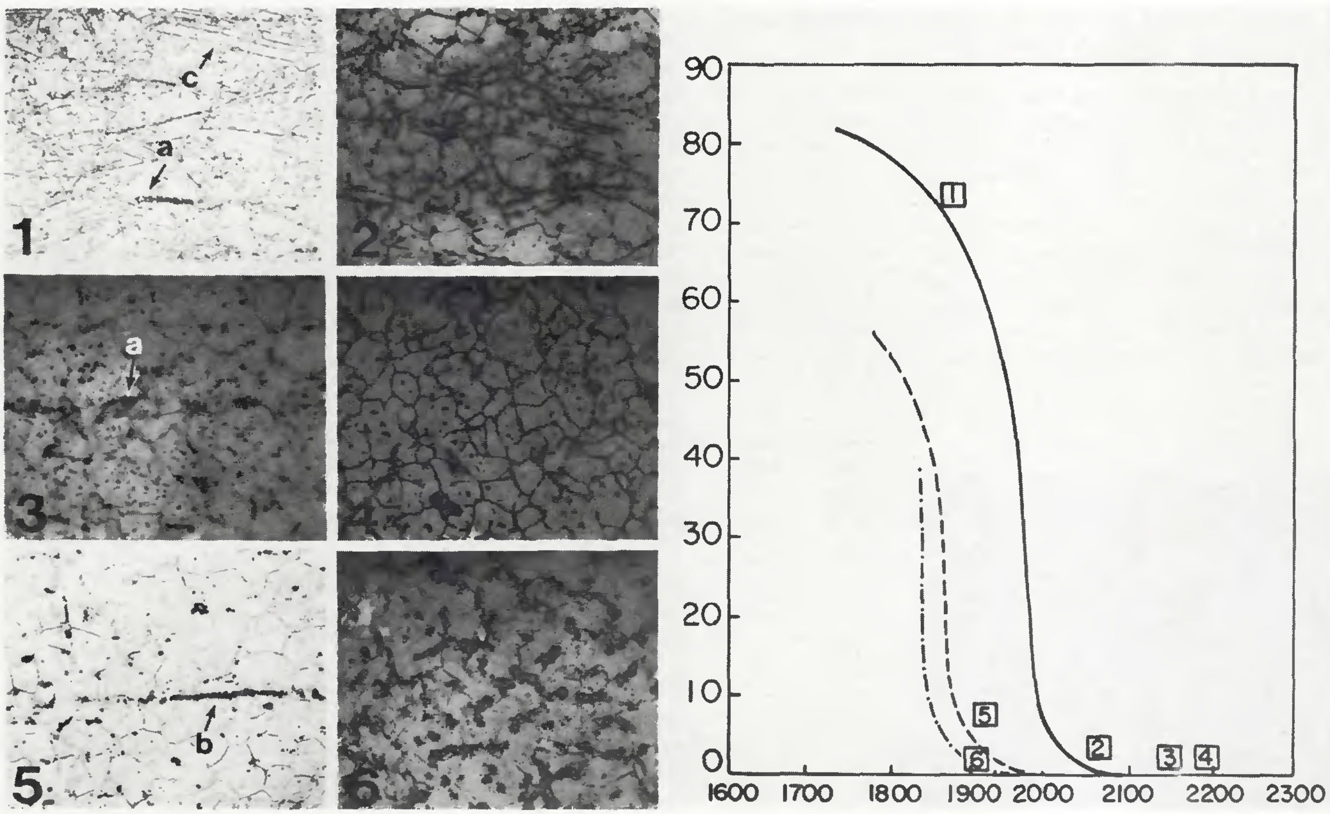

Fig. 7 — Microstructural evolution in solution annealed 718 during hot ductility test: 1. Quenched during heating at 1915°F, 2. Quenched during heating at 2070°F, 3. Quenched during heating at 2150°F, 4. Quenched during heating at 2170°F, 5. Quenched during cooling at 1920°F from a maximum temperature of 2130°F, 6. Quenched during cooling at 2035°F from 2190°F. °C = 5/9 (°F-32)

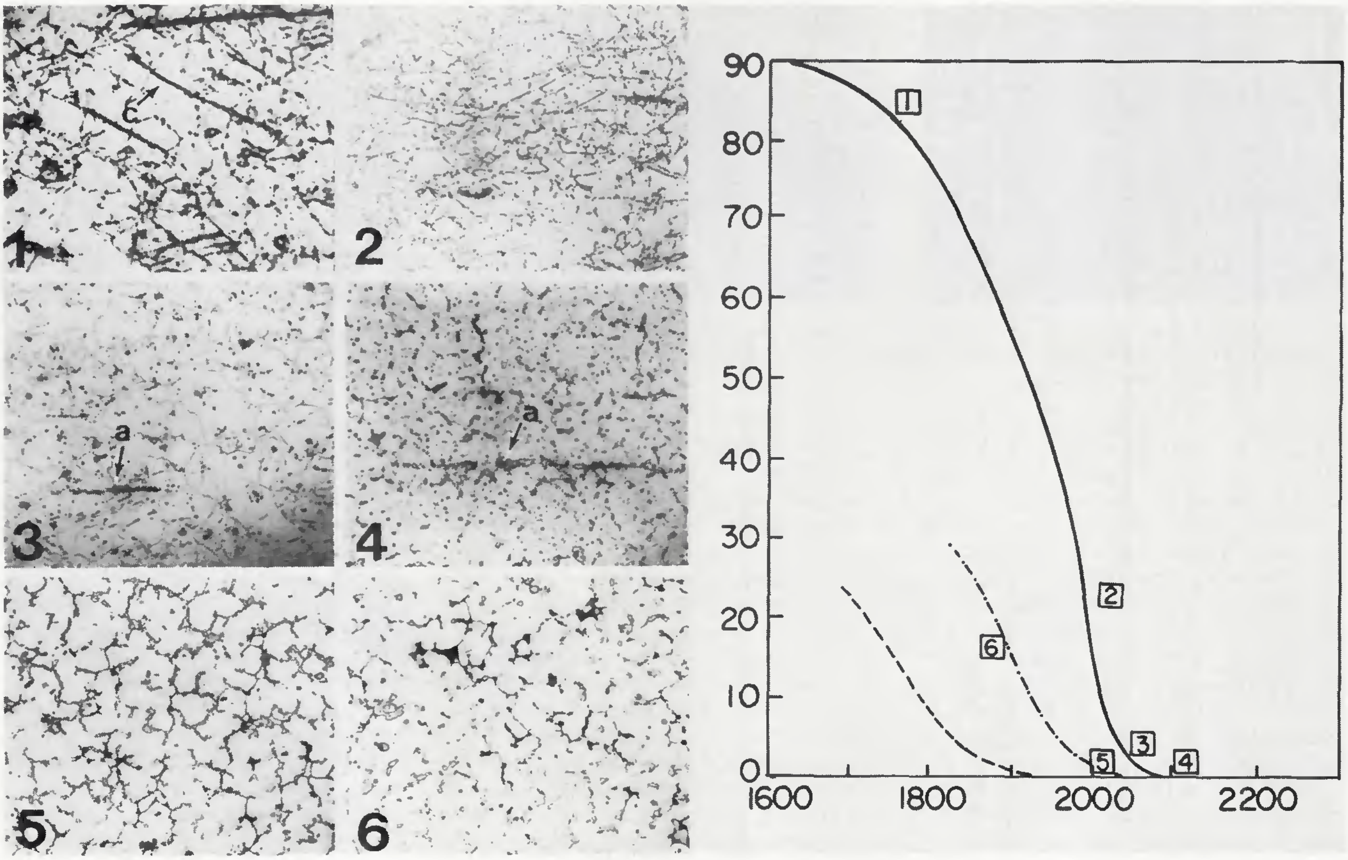

Fig. 8 — Microstructural evolution in age hardened 718 during hot ductility test: 1. Quenched during heating at 1790°F, 2. Quenched during heating at 2022°F, 3. Quenched during heating at 2050°F, 4. Quenched during heating at 2100°F, 5. Quenched during cooling at 2020°F from a maximum temperature of 2070°F, 6. Quenched during cooling at 1880°F from 2090°F. °C = 5/9 (°F-32)

Figure 13 shows a plot of ΔT_{NDT} vs. ΔT_{NbC} for the three heat treatments of this study. It was assumed that the incipient melting temperature was 2100°F (1149°C) in all heat treatments. Also shown in Fig. 13 are data taken from studies by E. G. Thompson (Ref. 26) and Duvall and Owczarski (Ref. 2), which were analyzed as in the present study. The data suggest that pretest heat treatment had the same relative effect on hot ductility test results whether the initial material condition was cold drawn wire filler metal, wrought plate, or a forging.

Discussion

The microstructures found in the 718 filler metal used in this study are not suggested to be optimum microstructures for plates or forgings which are to be joined by welding. The NbC and TiC stringers found throughout the microstructure resulted from the filler metal's drawing process. This process involved a 1950–2000°F (1066–1093°C) annealing step between draws. The anneal was sufficient to dissolve most phases except the carbides which were carried through the process, being drawn out during each reducing step. The stringers proved very helpful in locating and monitoring the liquation reaction. Not only did their size allow them to be observed with standard polish-and-etch metallographic techniques, but their directional orientation provided an internal marker from which to follow the development of intergranular liquation.

The difference in ductility loss during cooling between the three heat treatments of the present study was striking. However, the similarity in mechanisms

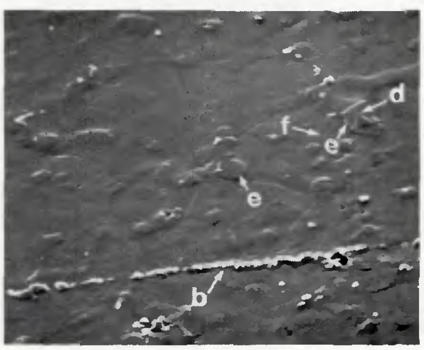

Fig. 9 — Formation of intergranular phase in as-received 718. "b" denotes typical unaffected TiC

Table 4—Summary of Phases and Their Contribution to Hot Cracking in Present Study

Constituent	Reaction to HAZ thermal cycle
γ'	Not observed
γ''	Not observed
Ni_3Nb	Dissolved during heating, not detrimental to ductility while cooling.
Laves	Not observed during heating, precipitated intergranularly during cooling, not believed to control ductility loss while cooling.
TiC	Did not dissolve/melt until after significant intergranular liquation had already occurred.
NbC	Melted by constitutional liquation mechanism, this melting initiated ductility loss while cooling.

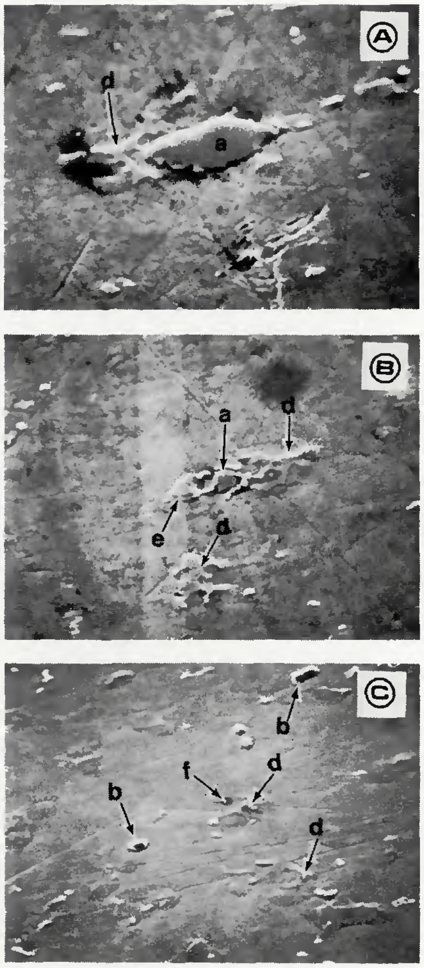

Fig. 10 — Dissolution of NbC and formation of intergranular phase in solution-annealed 718: A. — Initial stage of NbC dissolution during heating with Laves phase precipitated during cooling from Nb enriched region adjacent to carbide; B — NbC particles in advanced stage of dissolution during heating — large volume fraction of Laves phase precipitated during cooling from Nb enriched region adjacent to carbide; C — NbC particles fully dissolved during heating with Laves phase precipitated during cooling at locations of previous carbide — note TiC particles remain unaffected

which caused the ductility loss was just as striking. Constitutional liquation of NbC particles and the subsequent resolidification of liquated grain boundary regions is the key to understanding the HAZ hot cracking mechanism in alloy 718. Evidence of constitutional liquation was found in all three heat treatments as seen in Figs. 9–11; NbC particles "a" were observed to develop a transition zone "e" between themselves and the matrix. This transition zone contained two to three times the matrix level of Nb. As the temperature increased, the transition zone spread into the grain boundaries. It is hypothesized that micro-sized carbides and Laves phases situated in the grain boundaries also feed Nb into the grain boundary region.

Further evidence for constitutional liquation of Nb-rich particles can be found in the Ni-Nb phase diagram shown in Fig. 14. A Ni-Nb eutectic exists at 1175°C (2147°F). Note that this is the approximate temperature at which the NbC particles began to dissolve into the grain boundaries in the present study. Note also that such a eutectic requires approximately 50 wt-% Nb. Such a high Nb concentration could best be supplied by NbC particles.

The widened grain boundaries seen at higher temperatures (Figs. 9, 10, and 11) indicate that incipient melting experienced by the NbC particles spreads through the grain boundaries in the form of an intergranular liquid. As this liquid cooled, precipitates "d" formed in the center of the widened grain boundaries. Table 3 shows that the chemical composition of this phase was approximately that of the Laves phase. The location of this phase at the center of the widened boundary suggests it formed from the last liquid to solidify.

This freezing process can be rationalized for the binary case as in the modified Ni-Nb phase diagram of Fig. 15. The nonequilibrium solidification of the intergranular liquid is shown in the modified Ni-Nb diagram by dashed lines and a hypothetical Laves phase. As the intergranular liquid solidified, it could freeze either as composition range A or composition range B depending on the amount of Nb-dilution which occurred during melting. If the liquid froze as composition A, it would form a solid solution with no precipitates. If it formed in composition range B, it would form a divorced eutectic of nickel-niobium solid solution closest to the unmelted matrix and Laves precipitates near the center of the boundary region. Both types of grain boundaries were found in the present study, suggesting a wide range of compositions in the grain boundary regions throughout the microstructure. This was found in all three heat treatments.

The observation of Laves-type precipitates situated in the resolidified grain boundaries suggests several important points concerning a hot cracking mechanism. Note that all heat treatments produced essentially the same composition of intergranular Laves precipitate during cooling. This implies that all three heat treatments had intergranular liquid to the same minimum temperature during cooling. This minimum temperature is the Laves eutectic assuming the alloy to behave in a manner portrayed by Fig. 15 as suggested by the microstructure. The difference in hot cracking susceptibility due to heat treatment would not depend on the eutectic temperature of the intergranular liquid. This temperature would be constant. Instead, the differences in hot cracking susceptibility would depend on the amount and distribution of the intergranular liquid. The possible mechanisms controlling this distribution are discussed in the following paragraphs.

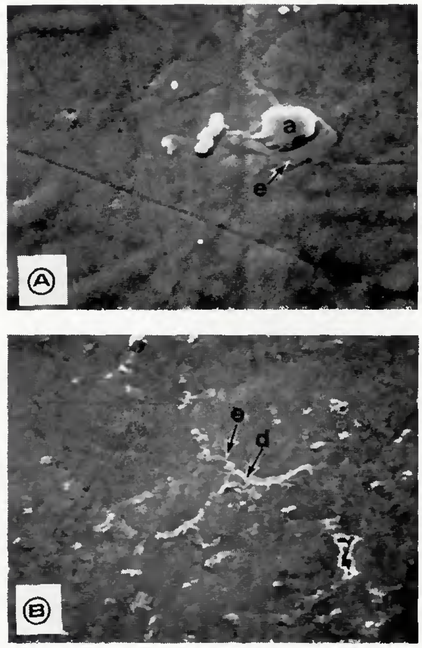

Fig. 11 — Dissolution of NbC and formation of intergranular phase in age-hardened 718: A — NbC dissolution during heating and formation of adjacent zone of high Nb concentration; B — formation of intergranular liquid at Nb enriched zone and subsequent intergranular wetting — Laves phase precipitated intergranularly on cooling in the form of divorced eutectic structure

Having discussed the similarities of intergranular melting and solidification in all three heat treatments of 718, Fig. 13 demonstrates the need to explain the dramatic differences in ductility loss during cooling as a function of heat treatment. Figure 13 clearly shows the need to explain why the ductility loss is greatly reduced by the SA treatment and why the AH treatment increases the ductility loss once again.

The answers to these questions rest in the amount and distribution of intergran-

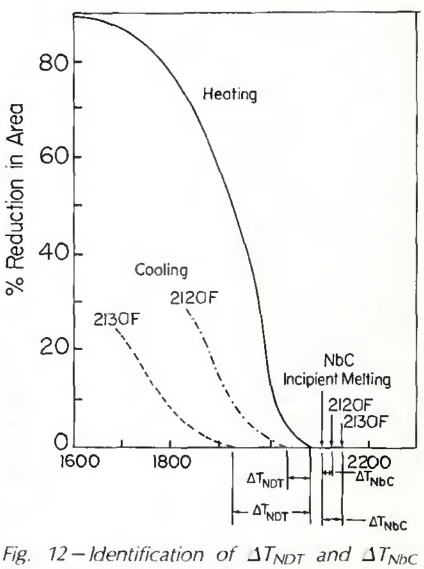

Fig. 12 — Identification of ΔT_{NDT} and ΔT_{NbC} from a typical hot ductility curve

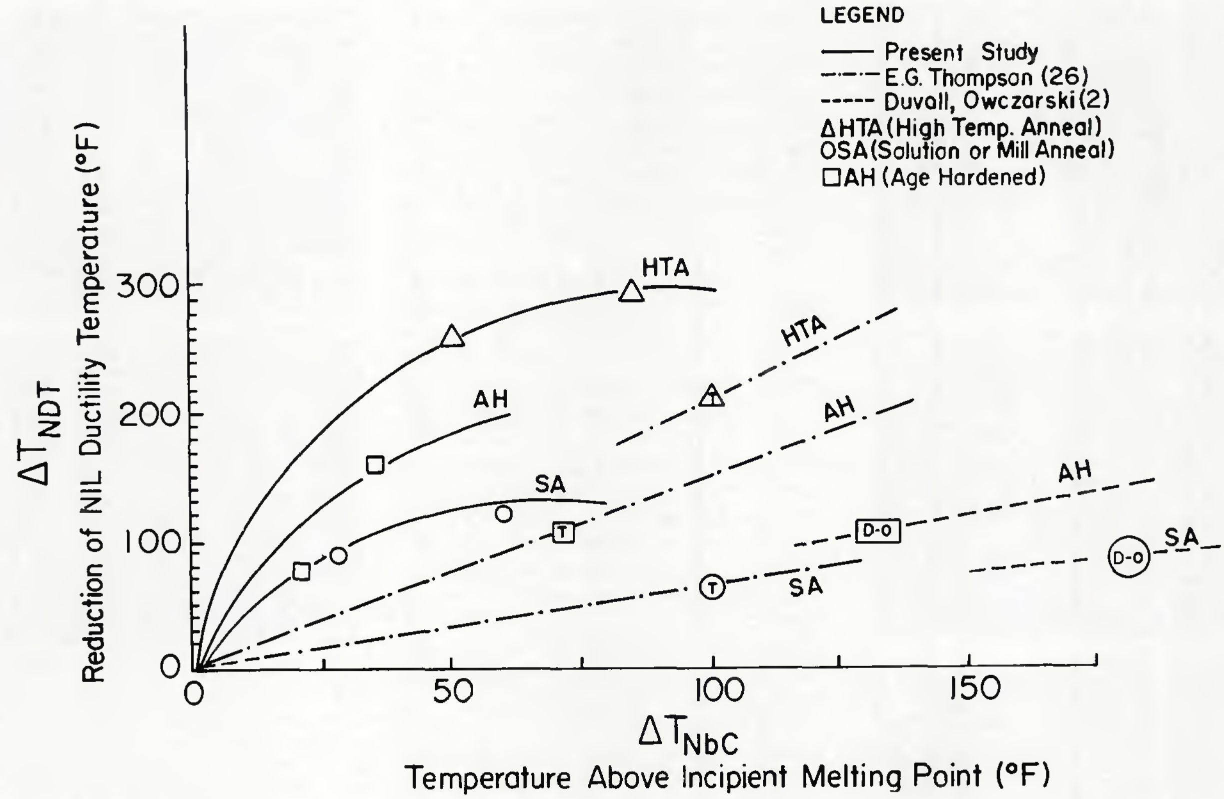

Fig. 13 — Ductility loss as a function of maximum temperature above NbC incipient melting

ular liquid, as a function of temperature, for each heat treatment. The amount of intergranular liquid is best discussed in terms of liquid volume per grain boundary area. The total volume of intergranular liquid, as a function of temperature, is dependent on intergranular chemistry. For the binary model of Fig. 15, this volume is dependent on the intergranular niobium content.

Two ideas have been set forth in the literature which suggest that the intergranular niobium content can be controlled by heat treatment. This could then explain the dependency of hot cracking on heat treatment. Lippold (Ref. 28) has pointed to the trapping of matrix Ti by grain boundaries during welding of alloy 800 as the cause of hot cracking in that alloy. Vincent (Ref. 27) has pointed to the possible trapping of matrix Nb by grain boundaries during welding of alloy 718 as a cause of hot cracking.

Although the present study has focused on the dissolution of NbC as a source for intergranular Nb, it is plausible that matrix Nb also contributes to the total intergranular Nb content. The availability and distribution of matrix Nb could explain the difference in ductility loss due to heat treatment.

Consider the AR material which had been annealed at 2000°F (1093°C). This heat treatment would have distributed Nb throughout the matrix by dissolving those phases which normally take Nb out of solution. The SA material on the other hand had Ni_3Nb precipitated heavily throughout the matrix. These precipitates did not dissolve until temperatures approached the incipient melting temperature. These precipitates could deplete the matrix of Nb which would otherwise be free to accumulate in the grain boundaries. Thus, it could be

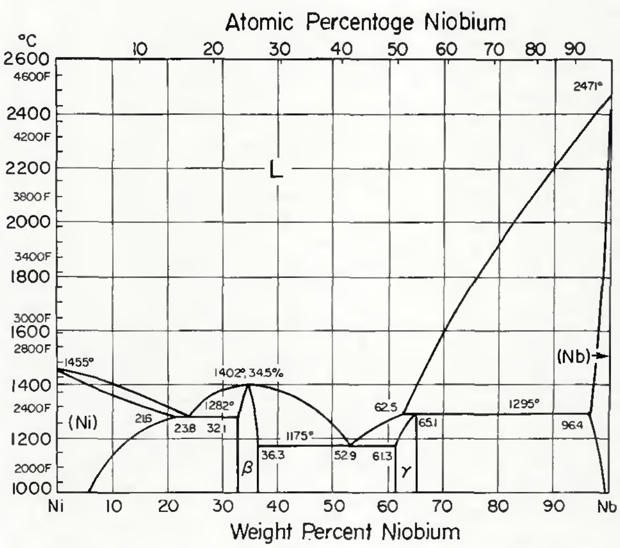

Fig. 14 — Ni-Nb phase diagram

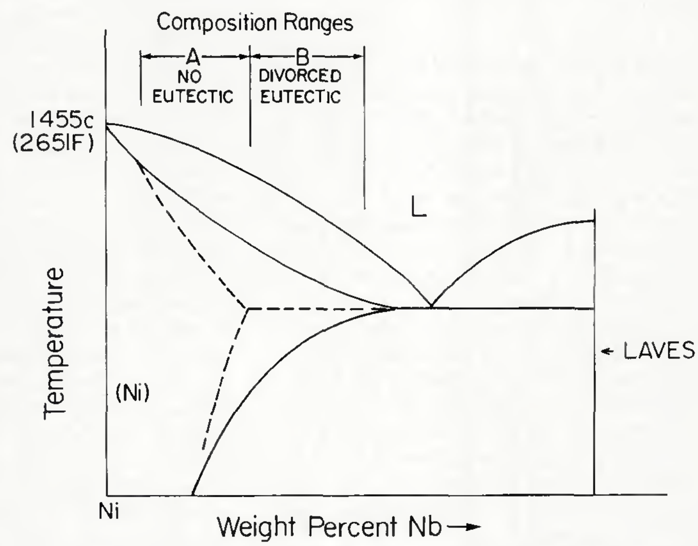

Fig. 15 — Hypothetical Ni-Nb phase diagram showing the development of divorced intergranular eutectic through segregation

argued that the AR material had a larger amount of free Nb available to accumulate in the grain boundaries than did the SA. This greater Nb content would then cause the AR material to be more crack sensitive by increasing the volume of liquid present.

The increased ductility loss of the AH material over the SA must also be considered. The AH heat treatment should take more Nb out of solution than the SA treatment due to precipitation and, according to the argument just presented, be less hot crack sensitive than the SA material. However, the AH condition exhibited a hot ductility response more crack-sensitive than the SA condition.

The cause of the increased hot crack sensitivity in the AH condition could come from two sources. One source of the increased hot crack sensitivity in the AH condition could be the precipitation of Nb-rich phases in the grain boundary. Airey (Ref. 29) found that precipitates formed semi-continuous grain boundary films under AH heat treating conditions in nickel-base alloy 600. The SA heat treating condition promoted large discrete precipitates. Figure 5 also suggests that the AH heat treatment would promote further precipitation of the NbC phase. These two things taken together suggest that the AH material possibly had a ready source of extra Nb present in the form of intergranular NbC precipitates.

Another cause for the heightened hot crack sensitivity in the AH condition could be the distribution of the intergranular liquid present. The AH condition would be more crack sensitive than the SA if the liquid wet the boundaries more in the AH condition (Ref. 16). Impurities such as phosphorus (Ref. 8) and sulfur (Ref. 8), when segregated intergranularly, are known to affect the wetting behavior of the liquid. Such impurities can also control the wetting behavior as a function of temperature (Ref. 8, 21-23). Airey (Ref. 29) found that phosphorus segregated more strongly to grain boundaries under AH conditions than during other heat treating conditions in alloy 600. Such differences in intergranular impurity content due to heat treatment would be expected to influence hot crack susceptibility as observed in the present study.

Further research is needed to define the role of impurity segregation during heat treatment in the hot cracking of high alloy metals. The distribution of alloying elements and their possible partitioning to HAZ grain boundaries during welding should also be studied closely. Finally, the role of grain size in promoting hot cracking must be defined. Such a grain size study is currently underway.

Conclusion

The present study shows that heat treatment significantly alters the hot cracking susceptibility of alloy 718 based on hot ductility test results. This study also revealed that hot ductility during cooling was not compromised until constitutional liquation of NbC particles was initiated in the microstructure. The mechanism of constitutional liquation initiating intergranular liquation and ductility loss during cooling was the same regardless of heat treatment. Laves-type phase compositions were found precipitated in liquated grain boundaries. These were seen to be an artifact of the cooling process and not directly related to differences found in the loss of ductility during cooling.

It was postulated that the role of heat treatment in determining the magnitude of ductility loss was related to its control over the amount and distribution of Nb available to the liquated grain boundaries. The experimental results neither confirmed nor denied this hypothesis but certain circumstantial evidence was presented in its support.

The possible role of impurity atom segregation during heat treatment was not ruled out as a mechanism for controlling ductility loss during cooling. Such control would result from modification of either the eutectic melting temperature or distribution of the intergranular liquid phase during cooling.

Acknowledgments

The authors wish to thank Drs. Carl D. Lundin and Brian J. Kruse for their assistance in performing the Gleeble tests and to Dr. D. Nicolas for assistance with SEM and EDS analysis. This study was partially funded by a University of Alabama in Birmingham, Faculty Fellowship Grant and partially funded under NASA contract NAS8-34962.

References

1. Nippes, E. F., and Savage, W. F., 1949. Developoment of specimen simulating weld heat-affected zones. *Welding Journal* 28(11):534-s to 546-s.

2. Duvall, D. S., and Owczarski, W. A. 1967. Further heat-affected zone studies in heat resistant nickel alloys. *Welding Journal* 46(9):423-s to 432-s.

3. Yeniscavich, W. 1966. A correlation of Ni-Cr-Fe Alloy weld metal fissuring with hot ductility behavior. *Welding Journal* 45(8):334-s to 355-s.

4. Weiss, B., Grotke, G. E., and Stickler, R. 1970. Physical metallurgy of hot ductility testing. *Welding Journal* 49:971-s.

5. Kreischer, C. H. 1963. A critical analysis of the weld HAZ hot ductility test. *Welding Journal* 42(2):49-s to 55-s.

6. Owczarski, W. A., Duvall, D. S., and Sullivan C. P. 1966. A model for HAZ cracking in nickel-base superalloys. *Welding Journal* 45(4):145-s to 155-s.

7. Savage, W. F., Nippes, E. F., and Miller, T. W. 1976. Microsegregation in partially melted regions of 70 Cu-30 Ni weldments. *Welding Journal* 55(7):181-s to 187-s.

8. Savage, W. F., Nippes, E. F., and Goodwin, G. W. 1977. Effect of minor elements on hot-cracking tendencies of Inconel 600. *Welding Journal* 56(8)245-s to 253-s.

9. Savage, W. F., and Dickinson, D. W. 1972. Electron microanalysis of backfilled hot cracks in Inconel 600. *Welding Journal* 51(11):555-s to 562-s.

10. Savage, W. F., Nippes, E. F., and Szekeres, E. S. 1976. A study of weld interface phenomena in a low alloy steel. *Welding Journal* 55(9):261-s to 268-s.

11. Phillips, R. H. 1980. Fractography and mechanisms of high-temperature cracking in ferritic steel weldments. *Metals Forum* 3:158.

12. Savage, W. F., Nippes, E. F., and Casteras, J. E. 1978. Effect of alloying additions on the weldability of 70 Cu-30 Ni. *Welding Journal* 57(12):375-s to 382-s.

13. Savage, W. F., Nippes, E. F., and Mushala, M. C. 1978. Copper-contamination cracking in the weld HAZ. *Welding Journal* 57(5):145-s to 152-s.

14. Savage, W. F., Nippes, E. P., and Mushala, M. C. 1978. Liquid metal embrittlement of the HAZ by copper contamination. *Welding Journal* 57(8):237-s to 245-s.

15. Pumphrey, W. I., and Jennings, P. H. 1948. A consideration of the nature of brittleness at temperatures above the solidus in castings and welds in aluminum alloys. *J. I. Metals* 75:235.

16. Smith, C. S., 1948. Grains, phases, and interfaces: an interpretation of microstructure. *Trans. A.I.M.M.E.* 175:175.

17. Williams, W. M., and Smith, C. S. 1952. A study of grain shape in an aluminum alloy and other applications of stereoscopic microradiography. *Trans. A.I.M.M.E.* 194:755.

18. Williams, J. A., and Singer, A. R. E. 1968. Deformation, strength and fracture above the solidus of temperature. *Journal of the Inst. of Metals* 96:5.

19. Borland, J. C. 1979. Fundamentals of solidification cracking in welds, part I. *Welding and Metal Fabrication* 47:19.

20. Rogerson, J. H., and Borland, J. C. 1963. Effect of shapes of intergranular liquid on hot cracking of welds and castings. *Trans. A.I.M.E.* 227:2.

21. Borland, J. C. 1961. Suggest explanation of hot cracking in mild and low alloy steel welds. *British Welding Journal* 8:526.

22. Bailey, J. A., and Tundermann, J. H. 1966. Effect of temperature on dihedral angle in some Al alloys. *Trans. A.I.M.E.* 236:1031.

23. Stickles, C. A. 1964. Some effects of temperature and hydrostatic pressure on interfacial tensions in nickel-lead systems. *Trans. A.I.M.E.* 230:20.

24. Stickels, C. A., and Hucke, E. E. 1964. Effect of stress on dihedral angle in leaded nickel. *J. I. Metals* 92:234.

25. Eiselstein, H. S. 1965. Metallurgy of a columbium-hardened and nickel-chromium-iron alloy. *Advances in technology of stainless steel and related alloys, ASTM STP* 369:62-79.

26. Thompson, E. G. 1969. Hot cracking studies of alloy 718 weld heat-affected zone. *Welding Journal* 48(2):70-s to 79-s.

27. Vincent, E. R. 1980. *The microstructure of welds in Inconel 718.* Department of Physics, University of Bristol, United Kingdom.

28. Lippold, J. C. 1983. An investigation of HAZ hot cracking in alloy 800. *Welding Journal* 62(1):1-s to 11-s.

29. Airey, G. P. 1980. Microstructural aspects of the thermal treatment of Inconel 600. *Metallurgy* 13:21.